

GT2011-4* \$, +

FLUID DYNAMIC DESIGN AND OPTIMIZATION OF TWO STAGE CENTRIFUGAL FAN FOR INDUSTRIAL BURNERS

C. Ferrari, M. Pinelli, P. R. Spina
Dipartimento di Ingegneria (ENDIF)
Università di Ferrara
Ferrara, Italy

P. Bolognin, L. Borghi
Baltur S.p.A.
Cento (FE), Italy

ABSTRACT

In this paper, the fluid dynamic design of a two-stage centrifugal fan for industrial burner application is presented. The design is carried out by means of an integrated 1D/3D numerical procedure based on the use of CFD simulations. The CFD simulations are used either at the preliminary design stage to choose among competitive one- or two-dimensional geometries and then to test the generated three-dimensional geometries. The results show how the different design choices could impact on the performance parameters and, finally, how the analysis of the various alternatives allows the determination of the overall geometry of a complete and performing two-stage centrifugal fan.

NOMENCLATURE

b	blade span
C_H	slip factor
D	impeller diameter
Δp	pressure difference (loss/rise)
H	total head
M_t	torque
N	rotational speed (as round per second)
n	rotational speed (as round per minute)
n_c	specific speed
p	total pressure
Q	volume flow rate
r	impeller blade radius
V_u	absolute velocity tangential component
W	impeller relative velocity
α	return channel geometrical angle
β	impeller flow angle
β^*	impeller geometric angle
η	total efficiency
ρ	density
ω	speed of rotation (as radiant per second)

Subscripts

0	eye section, total state
1	inlet section
2	outlet section
des	design
imp	impeller
max	dimension constraint
rc	return channel
st1	first stage
st2	second stage
c1	return channel first curve
c2	return channel second curve

INTRODUCTION

Large size burners (up to 8-10 MW) with aerodynamically stabilized flames are widely used in process and energy industry. These burners usually use centrifugal fans for combustion air feeding. In recent years burner manufacturers have shown a growing attention in the achievement of as high as possible performances in terms of head, achievable maximum flow rate and efficiency, while containing overall machine dimensions, energy consumption and noise. This target is truly challenging or impossible to reach since it requires to over-constraint the fan design and, thus, it is very difficult to define a geometry, which can satisfy all the requirements. Multi-stage turbomachinery can offer some advantage with respect to single stage ones, but their design requires not only an accurate aerodynamic design of both impeller and diffuser as a separate component, but also a careful aerodynamic matching between them. In addition, the shape of return channel has to be accurately designed in order to achieve good efficiency. While a number of studies exist on multi-stage compressors or blowers, multi-stage centrifugal fans for industrial applications are not widespread, above all because of manufacturing costs.

In this paper, the fluid dynamic design of a two-stage centrifugal fan for industrial burner applications is presented. The design is carried out by means of an integrated 1D/3D numerical procedure based on the use of CFD simulations. CFD has demonstrated to be a powerful tool also for the optimization of fans, which, up until now, was less utilized for this kind of machines. Comprehensive information on the use of CFD in centrifugal fan optimization can be found in [1]. In recent works, examples of advanced use of CFD regarding optimization of centrifugal fans can be found in [2] and [3]. In this paper, in order to perform the design of the fan, three main phases can be recognized:

- one-dimensional design. Starting from the required performances, the main characteristics of machine geometry are obtained, which are: the main dimensions (diameters, flow passage areas, etc.) and the blade mean line, which has to be defined in terms of shape along the impeller and of inlet and outlet angles. The impeller blade mean line and the inlet and outlet blade angles are determined with 1D criteria according to machine specifications. The subsequent 3D analysis can then be focused on a particular geometry and, thus, the parametric analyses can be optimized with respect to computational effort and time.

- preliminary simplified 3D simulations to choose among competitive one- or two-dimensional geometries. In this manner, a wide number of alternatives can be rapidly evaluated

- three-dimensional fluid dynamic numerical design. In this phase, the best alternatives identified in the previous phase are fully simulated and the three-dimensional geometry is optimized.

ONE-DIMENSIONAL DESIGN

The fan to be designed is used as air feeder in a 8 MW industrial burner based on aerodynamically stabilized flame. The fan must provide the necessary air flow rate for the combustion process and must be able to overcome the pressure losses along its path. In particular, the main sources of losses are due to the swirler and to the flame stabilizer. The fan design was part of a research project carried out in collaboration with the burner manufacturer, which specified the requested operating condition and the desired economic and geometric constraints. The target design conditions of the fan to be designed are then:

- volume flow rate $Q_{des} = 11000 \text{ m}^3/\text{h}$;
- total pressure rise $\Delta p_0 = 3700 \text{ Pa}$;
- rotational speed $n = 2850 \text{ rpm}$.

Moreover, the manufacturer asked to accomplish with some economic and geometric constraints. These constraints are:

- electric motor maximum power lower than 15 kW;
- maximum radial size lower than 480 mm;
- as low as possible axial space requirement.

As a first step, by simple elaboration, a target overall efficiency is evaluated. The calculated efficiency is equal to $\eta = 0.75$. By considering the electric motor efficiency, the fan efficiency should at least be about 0.80, which is value theoretically achievable but hardly reachable due to the external

diameter constraint. However, the efficiency to be used in the subsequent design was evaluated by means of classical statistical correlations: at this stage, the value of this efficiency - very dependent on the source - has only a statistical meaning. A sensitivity analysis revealed that the different values found for the total efficiency, which can range from 0.70 to 0.85, are within a band of about $\pm 15 \%$.

A tentative geometry was defined through geometry correlations as a function of the specific speed n_c . A literature survey was first carried out in order to assess the most reliable and most commonly used methods. In particular, the design proposed by Cordier [4], Wright [5], Stepanoff [6], Eck [7], have been analyzed. The preliminary tentative design resulted in a single-stage centrifugal fan geometry. By using the Cordier correlation, an external diameter $D_2 = 605 \text{ mm}$ was then obtained. The impeller eye diameter D_0 was instead estimated by means of the correlation proposed by Wright [5]

$$\frac{D_0}{D_2} = 1.53\varphi^{\frac{1}{3}} \quad (1),$$

where φ is defined by

$$\varphi = \frac{Q}{ND_2^3} \quad (2),$$

where N is the rotational speed in round per second. The calculation allowed the estimation of the impeller eye diameter as $D_0 = 338 \text{ mm}$.

Beside this approach, the results of the design by using the correlations include in Eck [7] were analysed. For the external diameter determination, Eck proposed a diagram very similar to the Cordier one, while for the impeller eye, the following correlation was used:

$$\frac{D_0}{D_2} \geq 1.194\varphi^{\frac{1}{3}} \quad (3)$$

In this case, φ is defined as

$$\varphi = \frac{Q}{u_2\pi D_2^2/4} \quad (4)$$

From this procedure, the two diameters resulted in $D_2 = 549 \text{ mm}$ and $D_0 = 379 \text{ mm}$. As can be seen, the values of the external diameters differ of less than 10 %, which, at this design stage, can be considered acceptable. Nevertheless, this radial size exceeded the constraint of a maximum radial size lower than 480 mm.

Hence, a two-stage fan using the above outlined correlations was designed. In this design, the partial machines must elaborate the same volume flow rate but has to supply only half of the total head. Even in this case, the calculated external diameter would exceed the constraint of a maximum size lower than 480 mm. Therefore, the design procedure was carried on by imposing the external diameter $D_{2max} = 480 \text{ mm}$. Since this is an over-constraint of the design, the one-dimensional procedure could not guarantee that the fan achieves the as highest as possible efficiency. Moreover, the statistical and empirical correlations could still be used, but an higher level of

uncertainty is to be expected. Hence, Eqs. (1) and (3) were applied by imposing the chosen external diameter and the impeller eye diameter D_0 resulted equal to about 338 mm.

The blade inlet diameter was chose equal to the impeller eye diameter, i.e. $D_1 = D_0 = 338$ mm. Hence, the inlet blade span b_1 was chosen according to Eck [7], who proposed the following equation

$$b_1 = \frac{D_1}{4\xi} \quad (5)$$

where ξ is a coefficient which stated if at the blade inlet the meridian velocity should be higher (accelerate), equal or lower (decelerate) with respect to the axial velocity.

Once the main dimensions were chosen, the meridian flow path was designed. To do this the following procedure was adopted. The inlet and outlet velocity ratio can be written as [5]

$$\frac{W_2}{W_1} = \left(\frac{b_1 r_1}{b_2 r_2} \right) \left(\frac{\sin \beta_1}{\sin \beta_2} \right) \quad (6)$$

By imposing the meridian velocity distribution in design conditions along the meridian channel, it is possible to calculate the outlet blade span b_2 . For instance, if the meridian velocity remain constant from inlet to outlet, it is possible to state that

$$b_1 r_1 = b_2 r_2 \quad (7)$$

A very critical parameter is the outlet blade angle β_2^* . To determine β_2^* , the relative velocity ratio was chosen according to the well known and established limit proposed by de Haller, which control the diffusion inside the blade passage

$$\frac{W_1}{W_2} > 0.72 \quad (8)$$

With this assumption, it is possible either (i) to calculate the outlet relative flow angle β_2 by imposing a value for the de Haller ratio or (ii) to impose a realistic value of β_2 and keep under control if Eq. (8) is satisfied. The outlet blade angle β_2^* is then calculated by means of a trial and error procedure which makes use of the slip factor correlation proposed by Stodola [8]

$$C_H = 1 - \frac{\frac{\pi \sin \beta_2^*}{Z}}{1 - \frac{V_{m2} \cot \beta_2^*}{U_2}} \quad (9)$$

and the formula for blade number estimation proposed in [7]:

$$Z = \frac{4\pi \sin \beta_2^*}{1.5 \left(1 - \frac{r_1}{r_2} \right)} \quad (10)$$

With this procedure, a number of geometries were generated. A first simulation campaign was performed as a initial coarse check on the tentative 1D geometries. These first trials demonstrated that the return channel could have significant pressure drops.

For this reason, a further design constraint was imposed on the impeller total pressure rise, which was increased by 20% for preventing the losses that can occur in the return channel.

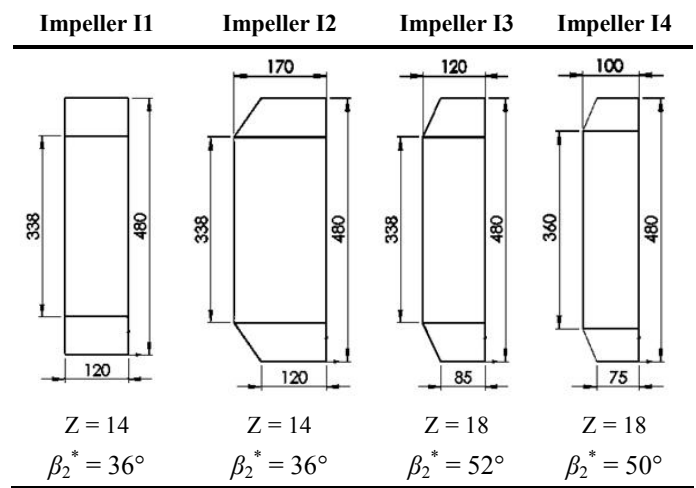


Figure 1 - One-dimensional geometries

Therefore, the design total pressure rise of each impeller must be higher than 2220 Pa. This design constraint, together with the external diameter constraint, substantially acted on the outlet blade angle β_2^* value and on the number of blade Z . The outlet blade angle is measured with respect to the tangential direction, and, for backward-curved blades, $\beta_2^* < 0$. Four geometries were finally chosen for the subsequent investigation. In Fig. 1, the main geometric parameters and the sketch of the meridian channel are reported. For the blade mean line design, the point by point methods of Pfeleiderer [9] was chosen. The adopted rule was a linear variation of the blade angle β between r_1 and r_2 .

In a two stage fan, the flow is guided from the outlet of the first impeller to the inlet of the second impeller by a return channel whose project required special attention because of geometric constraints imposed. The duct was designed by imposing the same velocity of the flow in each section. This was set in order to minimize the losses due to dramatic change of speed. The design of the midline of the stator vanes was made by using the point by point method of Pfeleiderer [9]. Fig. 2 shows the different trends in the angle $\alpha(r)$ used for the design. The angle α is the geometric angle of the blade return channel measured with respect to the tangential direction. The blade profile of RC1 and RC2 was obtained by imposing a curvilinear variation of $\alpha(r)$, while RC3 was obtained by imposing a linear variation of angle $\alpha(r)$ and RC4 was obtained by imposing a linear variation of the peripheral speed V_u .

NUMERICAL ISSUES

As stated in the previous paragraph, CFD simulation were used both at the preliminary design stage for the selection of the best geometries and for geometry optimization. The numerical simulations were carried out with the commercial CFD code ANSYS CFX 11.0 [10]. The code solves the 3D Reynolds-averaged form of the Navier–Stokes equations by using a finite-element based finite-volume method. A second-order high-resolution advection scheme was adopted to calculate the advection terms in the discrete finite-volume equations.

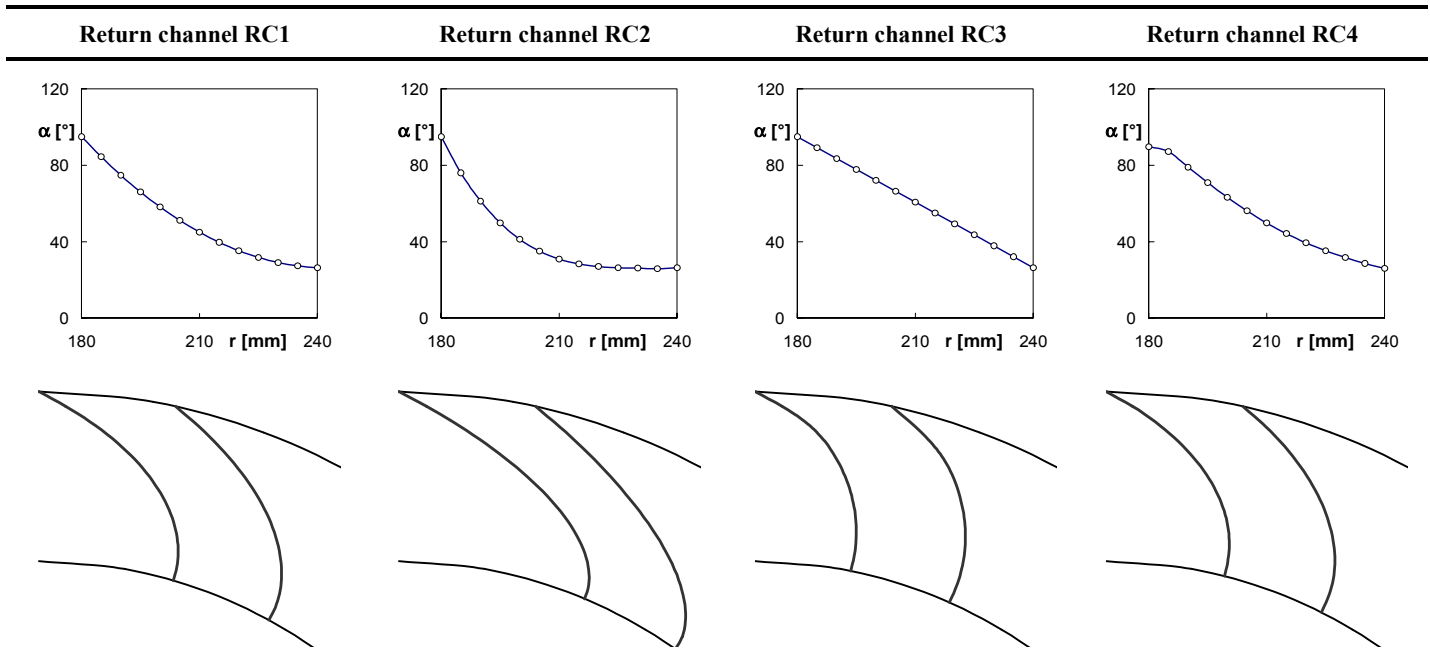


Figure 2 - Profile of $\alpha(r)$ used for the return channels (RC)

The grids used in the calculations were tetrahedral grids generated by means of ANSYS ICEM CFD 11.0 [11].

The standard two-equation $k-\varepsilon$ model was used to solve the turbulent flow. Near-wall effects is modeled by means of scalable wall functions based on the analytical-wall-function approach [12]. The simulations were performed in steady state conditions. When both stator and rotor are present in the simulation, the simulations are performed in a multiple frame of reference to take into account the contemporary presence of moving and stationary domains. In particular, a mixing plane approach was imposed at the rotor/stator interface. In this approach, a single-pass steady-state solution is calculated exchanging the flow field variables at the interface. Flow field data are averaged circumferentially for both frames of reference at the interface and passed to the adjacent zone as boundary conditions. This spatial averaging at the interface removes any unsteadiness generated in the zone-to-zone flow field, but the resulting solutions are often reasonable approximations of the time-averaged flow field.

Boundary conditions. To reduce computational effort, only a section of the full geometry has been modeled and, therefore, rotational periodic boundary conditions were applied to the lateral surfaces of the flow domain. A mass flow rate was imposed at the inflow boundary and an average relative static pressure p_{r2} was imposed at the outflow boundary.

CFD MODEL VALIDATION

The CFD model was validated with reference to a similar fan whose experimental characterization was available. In Fig. 3 the geometry and the impeller with a sample grid is reported. Three grids were generated: mesh 1, composed of 2'700'000 tetrahedral elements; mesh 2, composed of

2'800'000, and mesh 3, composed of 3'300'000 tetrahedral elements with prism layers added on blade surfaces in order to correctly solve the boundary layer. The mesh is divided as follow 43% of the total elements in the impeller domain, 32% in the volute domain and the remainder in the inlet domain. In Fig. 4, the curves of the total head of the impeller as a function of the volumetric flow rate calculated for the three grids are reported against the experimental one. The difference among the performance curves calculated for the three different grids are negligible, while the difference between computed and experimental performance curves can be considered acceptable, by also considering the good agreement between the shapes of the two curves and the geometric tolerances between the CAD model and the real geometry. Therefore, the CFD model was considered validated, and for the calculations reported in the following the first grid rationale was used, since it allows a lower computational effort than the other two grids, but with a comparable result accuracy.

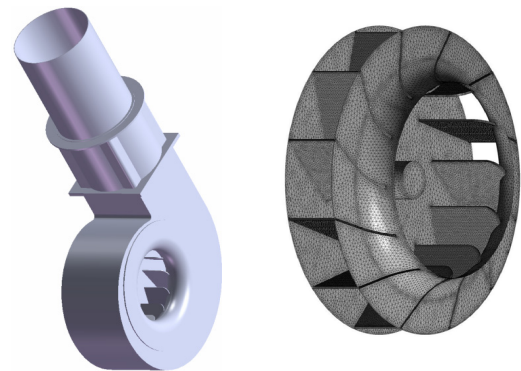


Figure 3 – Test geometry and impeller mesh

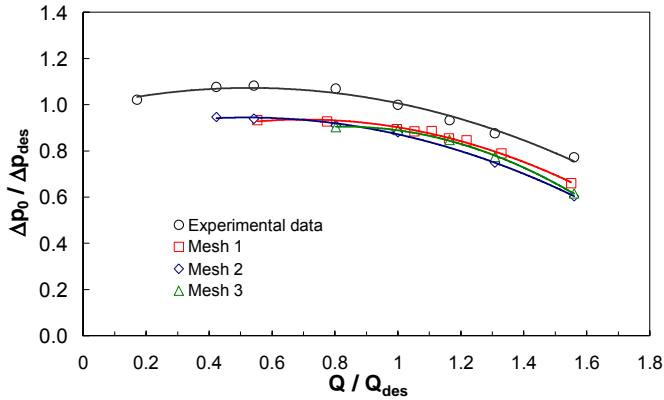


Figure 4 - Model validation: numerical and experimental performance curve

PRELIMINARY CFD ANALYSIS

Both the one-dimensional design of impeller and return channel were analyzed by simplified CFD numerical models in order to choose among the generated geometries.

The parameters calculated by the CFD are the pressure head and the efficiency η for each impeller designed with the one-dimensional procedure.

$$\Delta p_0 = p_{02} - p_{01} \quad (11)$$

$$\eta = \frac{\Delta p Q}{M_t \omega} \quad (12)$$

where p_{02} and p_{01} indicates the total pressure calculated in the outlet and inlet sections respectively and M_t is the torque acting on the impeller. The results are reported in Tab. 1. As can be seen from Tab. 1, each impeller allows a pressure rise Δp_0 higher than the value set for the one-dimensional design.

Results reported in Tab. 1 show that the impeller with the highest pressure rise is the I3, even though it is not the one with the highest efficiency. The impeller I4 has a lower pressure rise and efficiency but it has the advantage of a smaller axial space requirement.

Fig. 5 shows the pressure field for the 4 impellers resulting from CFD analysis. The related losses are due to the shape of

Table 1 – Pressure rise and efficiency of the four impellers

	Impeller I1	Impeller I2	Impeller I3	Impeller I4
Δp_0 [Pa]	2846	2880	3022	2508
H	0.95	0.94	0.92	0.88

Table 2 – Static and total pressure loss in the return channels

	Return channel RC1	Return channel RC2	Return channel RC3	Return channel RC4
Δp_0 [Pa]	396	323	345	316
Δp [Pa]	864	568	716	716

the leading edge, which is sharp instead of shaped with aerodynamic profiles, as for pumps or compressors. This is due to the fact that, in the case of fans, blades are often built by using metal sheet. The aerodynamic shaping and the edge rounding would lead to a substantial increase in costs.

As mentioned above, the design of the return channel was carried out by imposing a constant flow passage area, in order to minimize losses for abrupt changes in velocity. Vane midline has been tacked by changing the trend of $\alpha(r)$. The results are shown in Tab. 2 (which summarize pressure losses in the return channel) and Fig 6.

The losses are quite high for all the tested profiles. The minimum losses are obtained in the case of the profile obtained by setting a linear variation of V_u (RC4). As shown in Fig. 6, RC1 fails to sufficiently straighten the flow, while RC2 causes a flow almost completely separated over the entire blade.

The RC3 geometry allows a constant velocity flow, but the phenomenon of blockage at the outlet of the blade-to-blade channel causes an incomplete straightening of the flow. In the RC4 geometry, instead, the flow from the blade-to-blade channel is sufficiently straightened. This geometry is the one that allows the lowest losses, as above stated, although the blockage is still evident and there is an acceleration of the flow, which cause losses for the sudden change of the velocity.

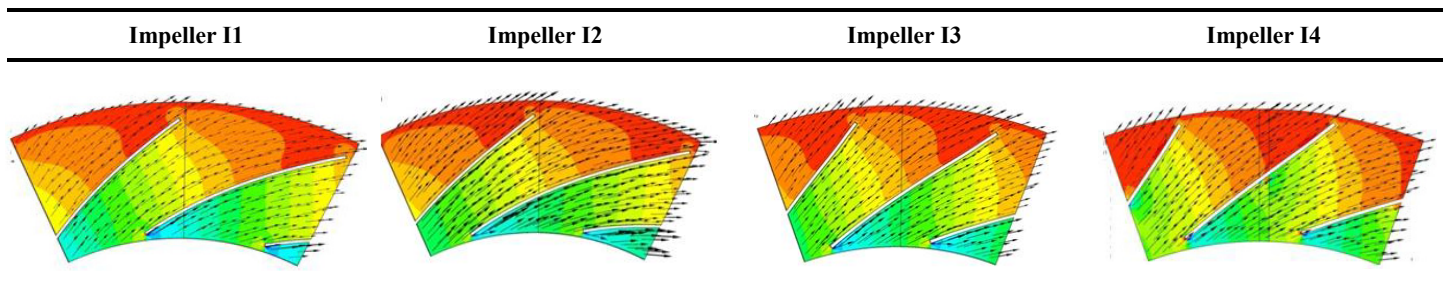


Figure 5 – Pressure gradient and velocity vectors for the four simulated impeller

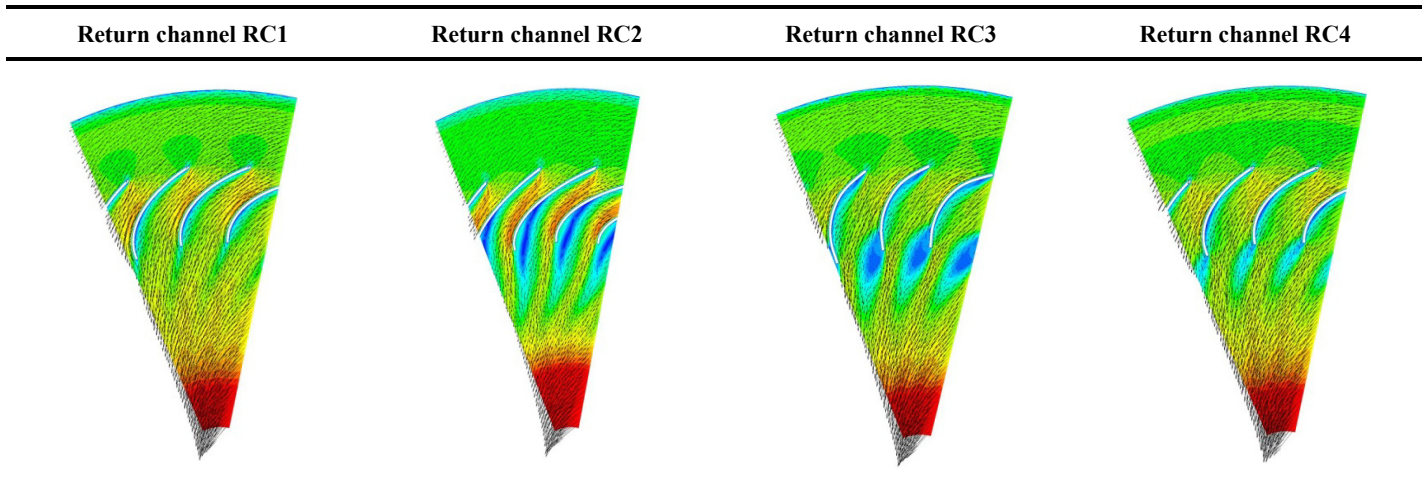


Figure 6 - Velocity profiles into the return channel

TWO-STAGE FAN THREE-DIMENSIONAL DESIGN

The complete three-dimensional model of the two-stage fan consists of an input volume, the first impeller, the return channel, the second impeller and an output volume. According to the analysis presented above, the impeller I3 and the return channel RC4 were chosen. As stated above, only a section of the full geometry has been modeled. In Figure 7, a sketch of the solid model of the first designed geometry is presented. The five elements, which compose the two-stage fan, are clearly noticeable. For the subsequent calculations, the volute was not modeled. In Fig. 8, a sample grid is presented.

A fully tetrahedral mesh was used. For the complete geometry simulation, a number of grid points ranging from 2'300'000 to 2'800'000 were used.

Figure 9 shows the velocity profile obtained from CFD. This first tentative geometry, which has the advantage of being very simple, proved to be not suitable to achieve the needed performance (results not reported). Therefore, a second modified geometry was proposed.

Results of these modifications are reported in Fig. 10.

Due to the fact that return channel size has been changed, also the impeller has been modified by substituting the impeller I3 (Fig. 9) with the impeller I4 (Fig. 10). This impeller has lower head rise and efficiency, as stated in Tab. 1. However, this choice was once again forced by geometrical constraint since the new designed return channel exceeded the overall axial space requirement. As can be seen, in the return channel, no stagnation or recirculation areas are highlighted and the entrance to the second stage seems to be characterized by only a little swirl component.

Even at the first stage, the speed is more uniform lowering the losses due to sudden changes in speed. According to these considerations, the pressure losses between the first and second stage of the fan are reduced to $\Delta p_{rc} = 653$ Pa. The power required by the impeller is 17.5 kW and it exceeds the constraint of a maximum power lower than 15 kW. The efficiency measured according to Eq. (12) is $\eta = 0.65$.

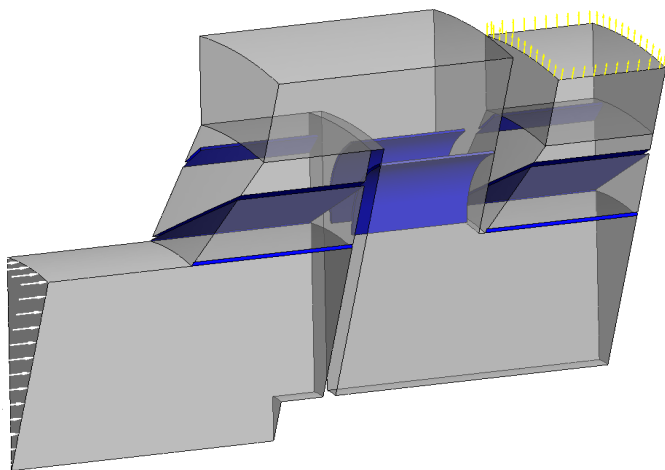


Figure 7 – Sketch of the two stage fan

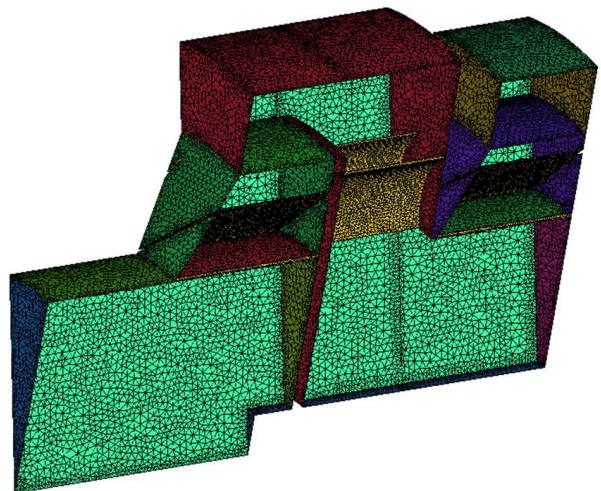


Figure 8 – Two stage fan numerical grid

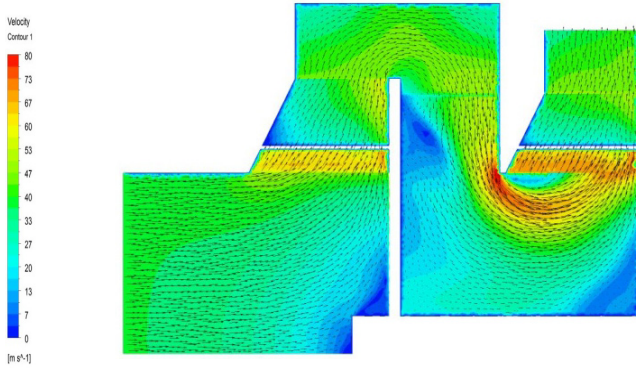


Figure 9 – Velocity along a complete cross-section geometry

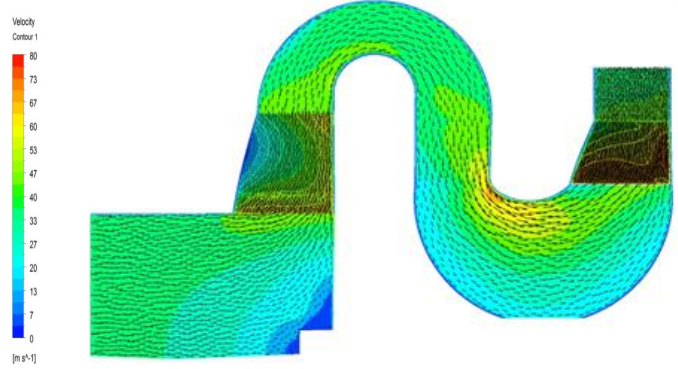


Figure 10 - Velocity along a complete cross-section geometry

To achieve the performance requested, an alternative return channel to be coupled with the impeller I4 was designed. In the new return channel the first curve is flattered, allowing the flow to have a more uniform velocity distribution in the ducts. The distance between the leading edge of the blades of the return channel and the axis of rotation is increased. This allows the flow to be straightened before it enters the second impeller. As can be seen from Fig. 11, this shape of the return channel allows the reduction of the rate of variation of the velocity in the first curve without causing flow detachment phenomena.

The velocity is also decreased in the second curve, even if a noticeable acceleration still remains especially in the inner side. It can be observed that this modification has led to an improvement in the uniformity of the flow along the entire machine.

The total pressure rises obtained with this new geometry were $\Delta p_{0st1} = 2668$ Pa, $\Delta p_{0st2} = 2415$ Pa for the first and second impeller, respectively. The pressure losses between the blade of the return channel were $\Delta p_{rc} = 561$ Pa, which are further reduced compared to the geometry of Fig. 9. The obtained efficiency is $\eta = 0.66$ and the power consumption rises to 20 kW. This figure exceeds by 5 kW the constraint of the maximum power lower than 15 kW.

In Fig. 12, the rendering of the final geometry is reported. For this final geometry, the performance curves were obtained by means of the same CFD methodology outlined above. In Fig. 13, the performance curves of the machine are presented. As can be seen, the requested design point can be considered attained, but the power consumption exceeded the constraint of a maximum power lower than 15 kW.

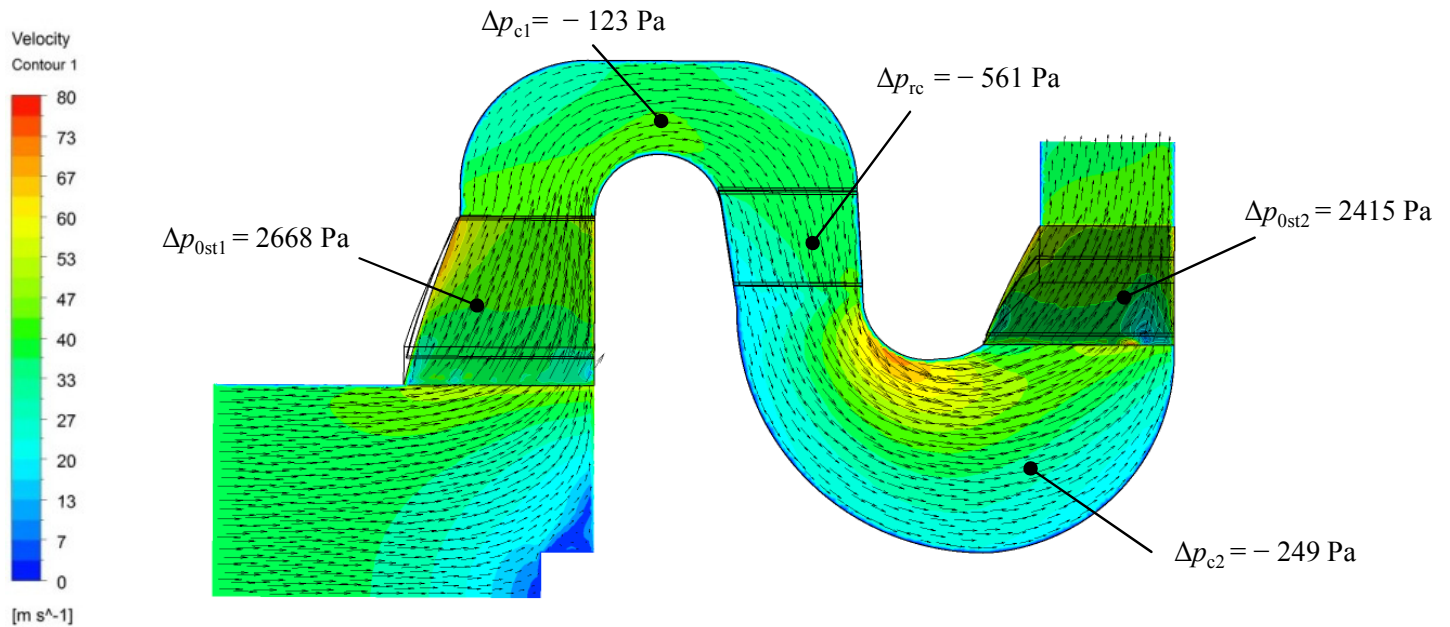


Figure 11 - Velocity and pressure drops along the two-stage fan

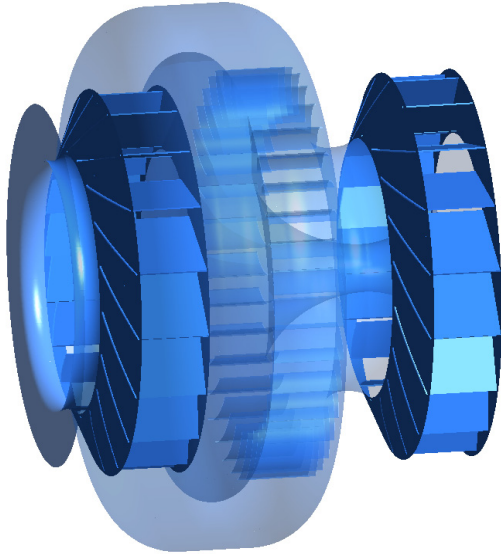


Figure 12 – Final two-stage geometry

Moreover, the best efficiency point is located at $Q = 8000 \text{ m}^3/\text{h}$, while the one-dimensional design value was originally $Q_{\text{des}} = 11000 \text{ m}^3/\text{h}$. This latter fact was due to the imposed constraints, which did not permit to fully comply with literature design criteria. It can also be highlighted, that the operating point is located in the central region of the curve where the efficiency ranges between 0.60 and 0.70. For the higher flow rates the efficiency of the machine drops abruptly because of the increase of the losses.

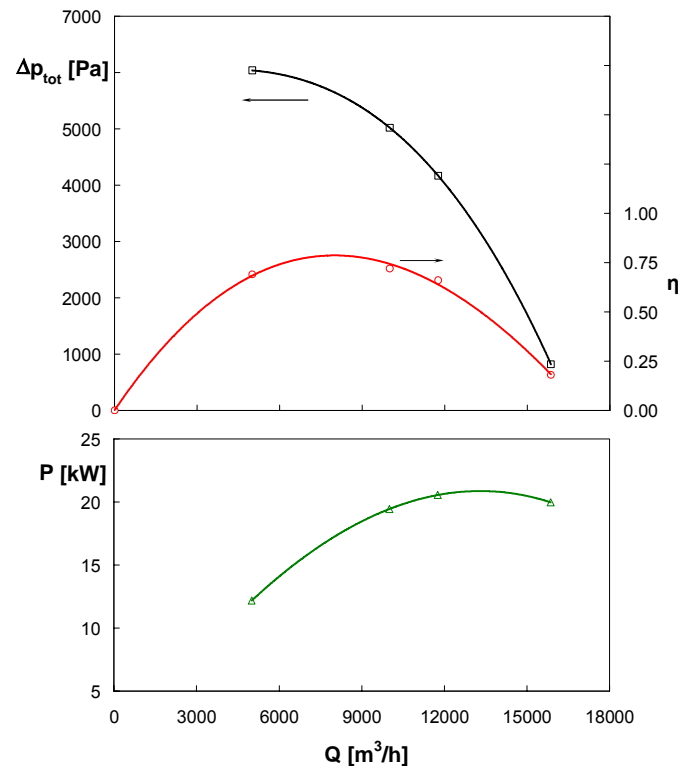


Figure 13 – Two stage fan numerical performance curves

CONCLUSIONS

In this paper, the fluid dynamic design of a two-stage centrifugal fan for industrial burner application is presented. The design is carried out by means of an integrated 1D/3D numerical procedure based on the use of CFD simulations. The CFD simulations are used either at the preliminary design stage to choose among competitive one- or two-dimensional geometries and then to test the generated three-dimensional geometries. The results show how the different design choices could impact on the performance parameters and, finally, how the analysis of the various alternatives allows the determination of the overall geometry of a complete and performing two-stage centrifugal fan.

ACKNOWLEDGMENTS

The authors gratefully acknowledge Prof. Roberto Bettocchi for the support during the project. The authors would like to thank Francesco Baraldo MSc for his valuable work in developing the geometrical model.

REFERENCES

- [1] Tallgren, J.A., Sarin, D.A., Sheard, A.G., 2004, Utilization of CFD in development of centrifugal fan aerodynamics, *C631/016/2004, Proc. International Conference on Fans*, IMEChE Publishing.
- [2] Younsi1, M., Bakir, F., Kouidri, S., Rey, R. 2007, Numerical and experimental study of unsteady flow in a centrifugal fan, *Proc. of the Inst. Mech. Eng., Part A: J. of Power and Energy*, 221 (7), pp. 1025-1036.
- [3] Yagnesh Sharma, N. and Vasudeva Karanth, K., 2010, Numerical analysis of a centrifugal fan for performance enhancement using boundary layer suction slots, *Proc. of the Inst. Mech. Eng., Part C: J. of Mech. Eng. Science*, 224 (8), pp. 1665-1678.
- [4] Cordier, O., 1953, *Ähnlichkeitsbedingungen für Strömungsmaschinen*, BWK Bd. 6, Nr. 10 Oktober
- [5] Wright, T., 1999, *Fluid machinery-Performance, analysis and design*, CRC Press.
- [6] Stepanoff, A. J., 1945, *Turboblowers. Theory, Design, and Application of Centrifugal and Axial Flow Compressors and Fans*, New York
- [7] Eck, B., 1973, *Fans*, Pergamon Press, New York.
- [8] Stodola, A., 1945, *Steam and Gas Turbines*, McGraw-Hill, New York
- [9] Pfleiderer, C., Petermann, H., 1972, *Strömungsmaschinen*, 4. Auflage, Berlin, Göttingen, Heidelberg: Springer-Verlag.
- [10] ANSYS CFX 11.0, 2007, *User Manual*.
- [11] ICEM CFD 11.0, 2007, *User Manual*.
- [12] Apsley, D., 2007, CFD Calculation of Turbulent Flow with Arbitrary Wall Roughness, *Flow, Turbulence and Combustion*, 78, pp. 153-175.